Morphological Disparity of the Humerus in Modern Birds

Francisco J. Serrano [1,2,3,*] **, Mireia Costa-Pérez** [4] **, Guillermo Navalón** [5,6] **and Alberto Martín-Serra** [3]

1   Real Academia de Ciencias Exactas, Físicas y Naturales, Calle Valverde, 22, 28004 Madrid, Spain
2   The Dinosaur Institute, Natural History Museum of Los Ángeles County, 900 Exposition Boulevard, Los Ángeles, CA 90007, USA
3   Departamento de Ecología y Geología, Facultad de Ciencias, Universidad de Málaga, Campus Universitario de Teatinos s/n, 29071 Málaga, Spain; almarse@uma.es
4   Departamento de Botánica y Geología, Universidad de Valencia, Calle Doctor Moliner 50, 46100 Burjassot, Valencia, Spain; mireiacostap@gmail.com
5   Department of Earth Sciences, University of Oxford, South Parks Road, Oxford OX1 3AN, UK; guillermo.navalon@earth.ox.ac.uk
6   Unidad de Paleontología, Departamento de Biología, Facultad de Ciencias, Universidad Autónoma de Madrid, Calle Darwin 2, Cantoblanco, 28049 Madrid, Spain
*   Correspondence: fjsa@uma.es

check for
updates

Abstract: From a functional standpoint, the humerus is a key element in the skeleton of vertebrates as it is the forelimb's bone that connects with the pectoral girdle. In most birds, the humerus receives both the forces exerted by the main flight muscles and the aerodynamical stresses exerted upon the wing during locomotion. Despite this functional preeminence, broad scale studies of the morphological disparity of the humerus in the crown group of birds (Neornithes) are lacking. Here, we explore the variation in shape of the humeral outline in modern birds and its evolutionary relationship with size and the evolution of different functional regimes, including several flight strategies, wing propelled diving and complete loss of wing locomotory function. Our findings suggest that most neornithines evolved repeatedly towards a general humeral morphology linked with functional advantages related with more efficient flapping. Lineages evolving high-stress locomotion such as hyperaeriality (e.g., swifts), hovering (e.g., hummingbirds) and wing-propelled diving (e.g., penguins) greatly deviate from this general trend, each exploring different morphologies. Secondarily flightless birds deviate to a lesser degree from their parent clades in humeral morphology likely as a result of the release from constraints related with wing-based locomotion. Furthermore, these taxa show a different allometric trend that flighted birds. Our results reveal that the constraints of aerial and aquatic locomotion are main factors shaping the macroevolution of humeral morphology in modern birds.

Keywords: Neornithes; humerus; allometry; avian flight; wing-propelled diving; flightlessness; geometric morphometrics

1. Introduction

With more than 10,000 living species occupying almost every habitat over the globe, birds are one of the most speciose and ecologically diverse group of vertebrates [1]. This extraordinary diversity is coupled with a wide range of physiological and morphological adaptations to locomotion, primal among which is aerial locomotion [2–4]. Most birds have wings capable of generate the necessary lift and thrust in the air to achieve some kind of flight [4,5]. Some birds have adapted to generate those forces underwater (i.e., wing-propelled diving), what in the case of penguins and some extinct auks

have involved the loss of flight capacity [6,7]. Other birds have lost the wing function completely, either in case of species adapted to terrestrial foraging (e.g., ratites, dodo), and those adapted to aquatic foraging through foot-propelling (e.g., flightless cormorant).

Proportions and cross-sections of forelimb bones studied within a phylogenetic context have shown a good correlation with wing-propelled locomotion [8–11]. During flight and wing-propelled diving the forces from the fluids (i.e., air and water, respectively) are exerted on the wing as bending and torsional moments which are transmitted from distal to proximal skeletal elements [5]. Hence, the humerus—the most proximal element of the forelimb—supports most of the wing stresses ultimatetly transferred through the elbow joint. In addition, the proximal epiphysis of this bone bears the attachment areas for the major flight muscles. Namely, the main muscles of downstroke (i.e., pectoralis) and upstroke (i.e., deltoideus and supracoracoideum) are inserted in the dorsal face of this epiphysis, while the main flexor of the wing (i.e., biceps) is attached to the ventral face [12,13]. All these features indicate that the humerus might be a key element to explore the link between skeletal morphology and locomotion throughout the evolution of the crown birds (i.e., Neornithes).

Our understanding of major morphological transformations over avian macroevolution has significantly improved in the last years with studies targeting several elements across the avian skeleton such as the skull [14–20], the girdles [20,21], the appendicular skeleton [22–24], and specifically the humerus among Mesozoic non-neornithine birds [25]. Despite the functional importance of the humerus and the remarkable morphological disparity displayed by this element in crown birds [26] (Figure 1), studies exploring this issue fall in one of two categories; (1) allometry using linear relationships between bone chord length, midshaft dimensions and body mass [27–30], or (2) using more complex methods but restricted to a particular clade and/or region of this bone [25,31]. However, a phylogenetically broad study of humeral morphology is lacking. Our study aims to fill this gap shedding light on the morphological transformations underwent by this bone over neornithine evolution.

Here we used geometric morphometrics to explore the morphological disparity of the humerus in birds across all the crown group of modern birds including one outgroup. Geometric morphometrics allows multidimensional analyses of the biological shape including compelling visualization of morphological differences in size and shape of anatomical structures [15,32]. Variations in the humeral morphology are assessed across a well-resolved phylogeny of Neornithes [33], which allows to explore those morphological patterns that are associated with changes in the wing function (i.e., from flight to diving), as well as with the reduction of the function (i.e., from flight to flightless).

Figure 1. Humeri in caudal view for selected taxa. (**A**) *Oxyura jamaicensis* UWBM 33103. Abbreviations: bc, bicipital crest; ch, caput humeri; dc, dorsal condyle; dpc, deltopectoral crest; fpn, fossa pneumotricipital; fp, flexor process; vc, ventral condyle. (**B**) *Haliaeetus leucocephalus* UWBM 33937. (**C**) *Macronectes giganteus* UWBM 38048. (**D**) *Nannopterum harrisi* LACNHM 89910. (**E**) *Hirundapus caudacutus* UWBM47345. (**F**) *Uria aalge* UWBM 79468. (**G**) *Fratercula corniculata* LACNHM 96912. (**H**) *Meleagris gallopavo* UWBM 59381. (**I**) *Casuarius bennetti* LACNHM 107030. (**J**) *Spheniscus humboldti* UWBM 81776. (**K**) *Columba rupestris* UWBM 59986. (**L**) *Cinclus mexicanus* UWBM 50254. Scale bars equate to 10 mm.

2. Material and Methods

2.1. Data Acquisition

Our data includes the humeri of 153 species encompassing 71 families and 23 orders within Neornithes. Species were classified according to the locomotory function of the wing as: (1) flight; (2) flight and diving; (3) diving; (4) and reduced function (Figure 2). Humeri were photographed directly in the collections of Natural History Museum of Los Ángeles County (Los Ángeles, CA, USA) and Burke Museum (Seattle, WA, USA). Photographs were taken from the caudal side of the bone following a standardized protocol for avoiding lens distortion and parallax [34]. The sample includes the cassowary (*Casuarius bennetti*) but other flightless Paleognathae as *Struthio camellus* and *Rhea americana* could not be analyzed because of the impossibility to locate enough landmarks on their humeri as this element is very modified in this taxa. Our sample also includes three recently extinct species: two auks (i.e., *Pinguinus impennis* and *Mancalla milleri*) assigned to diving category, and the dodo (i.e., *Raphus cucullatus*) assigned to the category of reduced wing function. The humeri of *P. impennis* LACNHM 90052 and *M. milleri* LACNHM 2813 were photographed from the collection of Natural History Museum of Los Ángeles County (Los Ángeles, CA, USA), while the humerus of *R. cucullatus* NHMUK PVA u/r was sourced from [35]. Finally, the Late Cretaceous ornithurine *Ichthyornis dispar* was included as outgroup of Neornithes [36]. The specimen *I. dispar* MUZ 689 was taken from [37].

We built a phylogenetic tree using the software Mesquite v.3.5 [38] extracting the topology and branch length information [33]. For clades not included in the [33], the information was obtained from specific references given from Timetree.org [39].

Individual values of body mass (M_b) were available for most of the extant birds specimens (n = 140; see Table S1). For those specimens with no individual information we obtained species' mean values of M_b from online databases [40,41]. We estimated the M_b of *I. dispar* from the alometric equation of the humeral length in [42]. Mass values for the other extinct birds were obtained from the femur, as this bone correlates better with the M_b than the humerus in flightless species [43]. M_b of *M. milleri* was estimated using the mean value of femoral lengths provided by [44] and the allometric equation in [42]. Likewise, M_b of *P. impennis* and *R. cucullatus* were taken from the mean values given in [43] and [45], respectively.

2.2. Analyses

A series of 19 homologous landmarks and three semilandmark strings (equidistant sliding semilandmarks) were digitized and scaled in each the images of humeri using tpsDig v.2.25 [46]. This was aimed to fully capture the outline shape of this element as well as the relative position and shape of the pneumotricipital fossa (Figure 3, Table S2). The raw X and Y coordinates of these landmarks and semilandmarks were imported into R environment [47] where all downstream analysis were conducted using the package geomorph v.3.1.3 [48].

Generalized Procrustes Analysis was carried out to remove differences in size, translation and rotation in the raw coordinates and extract shape data [49]. Sliding semilandmarks were optimized following a criterion of minimum bending energy [50]. Procrustes coordinates (shape) and log-transformed centroid size (i.e., a geometrically defined proxy of size *CS*) were obtained from this analysis. The relationship between the *CS* of the humerus and M_b in birds was explored within a phylogenetic context using a PGLS procedure (*procD.pgls*) [51], with log-transformed *CS* as dependent variable and log transformed M_b as independent variable. Two linear measurements traditionally used as estimates of size were calculated: humeral length (*HL*; L3 to L15) and midshaft width (*HW*; L11 to L12). The relationship between M_b and the size estimators of humerus, *HL* and *HW*, was tested using the same procedure. In addition, a linear model (*lm* function) was also fitted to calculate the slopes for the total sample of birds, and for flying and flightless subsamples separately. Afterwards, the allometric variation of shape was assessed through two Procrustes ANOVAs within a phylogenetic context using *CS* and M_b as

independent variables, respectively. Differences among flighted and flightless birds were also evaluated. Statistical significance of Procrustes ANOVAs was tested through non-parametric permutation tests (999 iterations) [51]. This non-parametric ANOVA is less likely to result in a type I error for data that violate the parametric assumptions but it might increase the likelihood of a type II error [51].
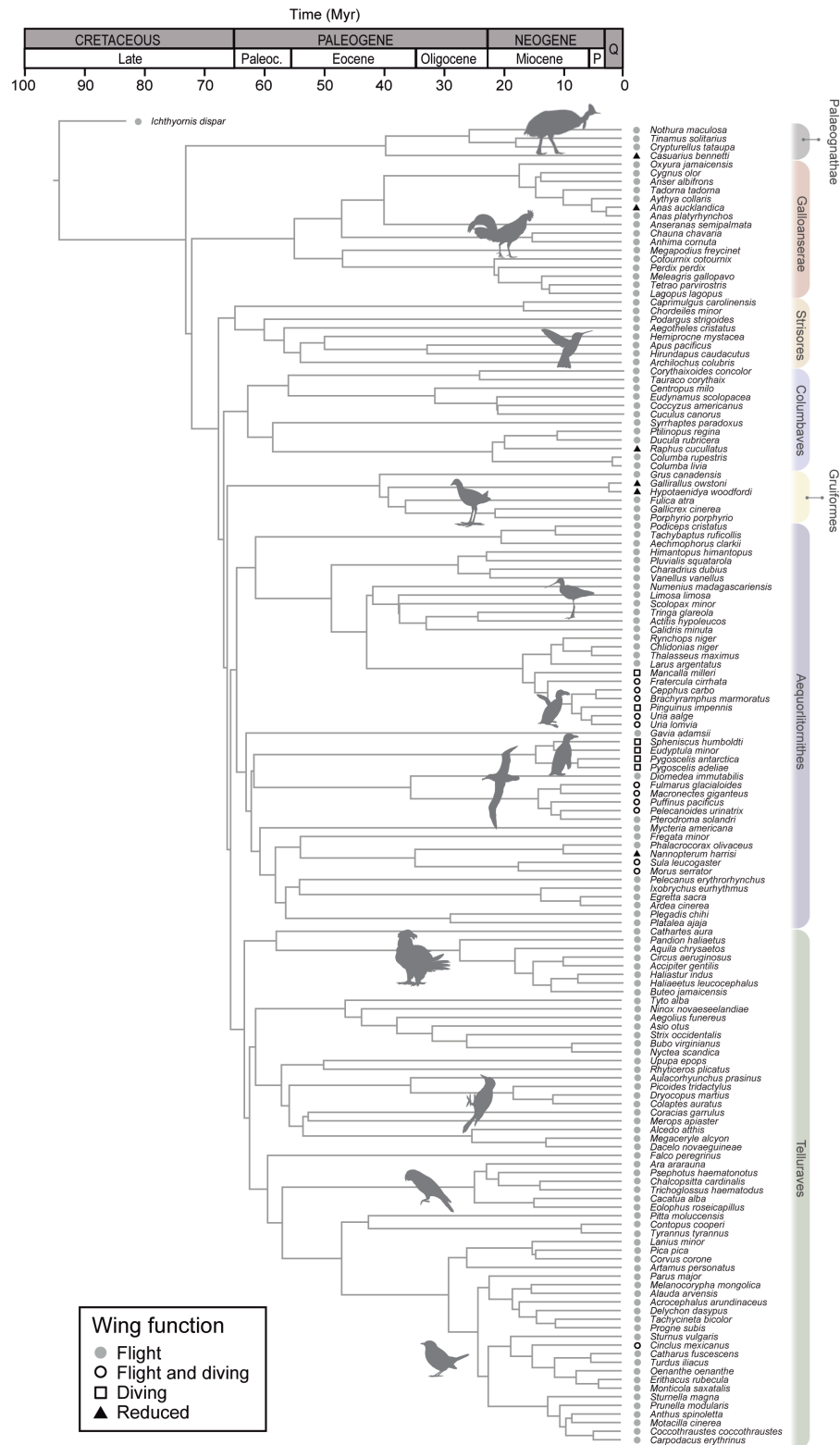

Figure 2. Time-calibrated phylogeny of the avian species used in this study (based on [33]) and their corresponding wing function categories.

Finally, the residuals obtained from the Procrustes ANOVA linear regression of shape against centroid size were incorporated as allometric-free shape coordinates in a principal components analysis (PCA; *plotTangentSpace*) to explore the main directions of morphological change. The morphological changes associated with the PCs were represented using *plotRefToTarget* function. The phylogeny was also incorporated into PCA visualization by generating phylomorphospaces using functions from *phytools* package [52]. This reconstructs the ancestral states of humeral shapes using squared-change parsimony [53]. Finally, to inform on the degree in which shape similarity associates with phylogenetic relationships we calculated K_{mult} using the function *physignal* also from geomorph. Values of $K_{mult} = 1$ represents the value of expected phenotypic similarity under a single-rate Brownian motion model of evolution; therefore, values $K_{mult} > 1$ indicate that related taxa are more similar to each other than expected under Brownian motion; while values of $K_{mult} < 1$ indicate that related taxa are less similar to each other than expected under a Brownian motion model of evolution.
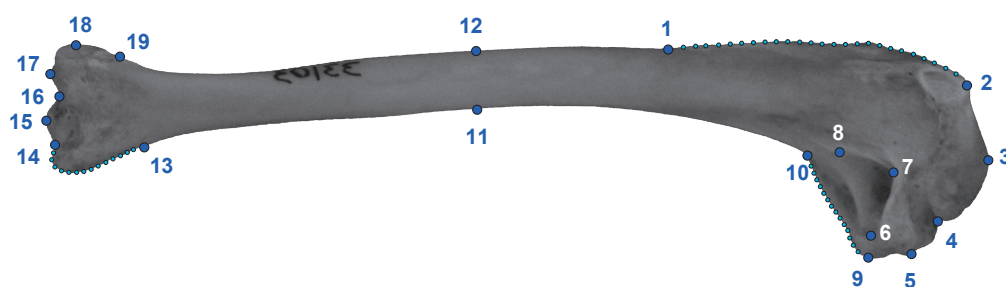

Figure 3. Humerus of *Oxyura jamaicensis* in caudal view showing the location of the 19 landmarks and the 3 strings of semilandmarks used in this study. Landmarks are described in the Table S2.

3. Results

Size metrics of the humerus (i.e., *HL*, *HW* and *CS*) correlate significantly with M_b (Table 1; Figure 4). Bivariate regressions of *HL* and *CS* provide almost identical results. Analyses using the three metrics report higher slopes for flying than for flightless birds, although the difference is smaller in the case of *HW*. Among flying birds, the slopes of *HL* and *CS* are higher than the slope provided by *HW*. Conversely, the slope from *HW* is steeper in the flightless subsample. PGLS evidences that these differences are highly significant ($p < 0.001$) and independent from the phylogenetic relationships (Table 1).

Table 1. Summary of bivariate regressions of body mass (M_b) on humeral size metrics.

Variable	Linear Model	adj R^2	*p*-Value	slope
CS	all birds	0.811	<0.001	0.423
	flighted	0.907	<0.001	0.484
	flightless	0.329	0.03	0.138
HL	all birds	0.824	<0.001	0.423
	flighted	0.915	<0.001	0.482
	flightless	0.340	0.027	0.145
HW	all birds	0.906	<0.001	0.365
	flighted	0.937	<0.001	0.379
	flightless	0.436	0.012	0.291

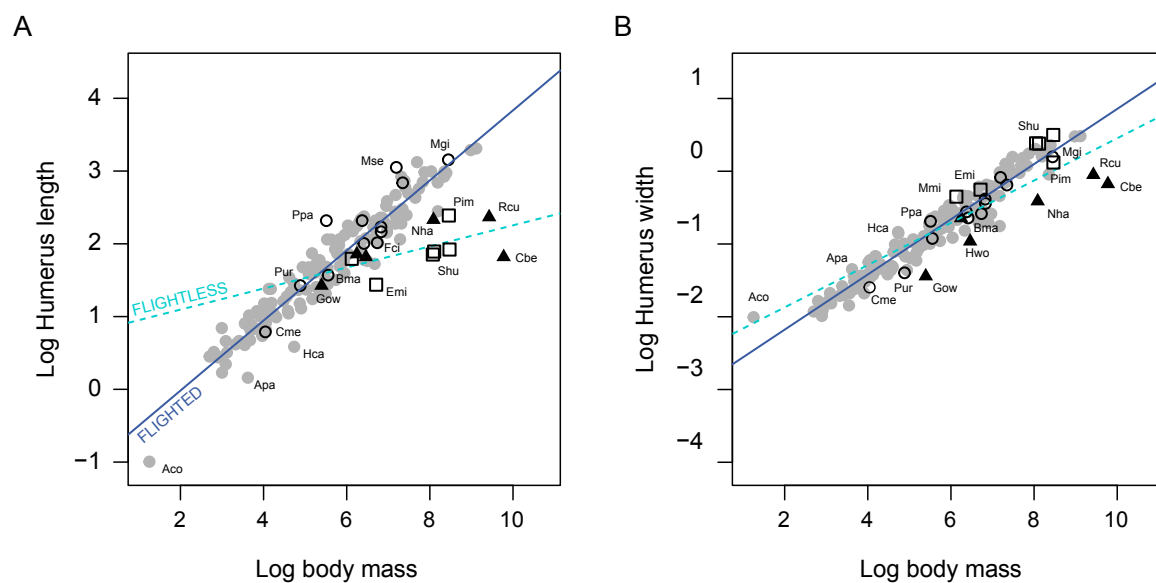| Variable	PGLS	adj R^2	*p*-Value
CS	M_b	0.370	<0.001
	flighted-flightless	0.099	<0.001
	M_b: flighted-flightless	0.259	<0.001
HL	M_b	0.387	<0.001
	flighted-flightless	0.092	<0.001
	M_b: flighted-flightless	0.260	<0.001
HW	M_b	0.495	<0.001
	flighted-flightless	0.016	0.014
	M_b: flighted-flightless	0.148	<0.001

Figure 4. Scaling of classic linear measurements of the humerus, length (**A**) and width at midshaft (**B**) on body mass. Symbols' shape corresponds with the function of wings given in Figure 2. Abbreviations: Aco, *Archilochus colubris*; Apa, *Apus pacificus*; Bma, *Brachyramphus marmoratus*; Cbe, *Casuarius bennetti*; Cme, *Cinclus mexicanus*; Emi, *Eudyptula minor*; Fci, *Fratercula cirrhata*; Gow, *Gallirallus owstoni*; Hca, *Hirundapus caudacutus*; Hwo, *Hypotaenidya woodfordi*; Mgi, *Macronectes giganteus*; Mmi, *Mancalla milleri*; Mse, *Morus serrator*; Nha, *Nannopterum harrisi*; Ppa, *Puffinus pacificus*; Pim, *Pinguinus impennis*; Pur, *Pelecanoides urinatrix*; Rcu, *Rapphus cucullatus*; Shu, *Spheniscus humboldti*.

Multivariate regressions of shape coordinates on M_b and CS reveal that the allometric variation of humeri is significant but small: M_b explains 2.2% of the total variance, while CS explains 5.8% (Table 2). The morphological variation associated to M_b show that heavier birds tend to have longer and slenderer humeri (i.e., less robust) as compared to lighter birds (Figure 5A). Similarly, the allometric change regarding CS shows that small humeri are more robust than larger humeri (Figure 5B). Differences between flying and flightless birds were not statistically significant (M_b: $p = 0.074$; CS: $p = 0.108$). However, visual observations reveal that the allometric pattern associated with M_b seems to be reversed in flightless birds with more robust humeri associated with heavier birds (Figure 5A). Importantly, although swifts and hummingbirds exhibit much stouter humeri than the rest of birds, the results for allometry were the same when these birds were removed from the analyses (Table S3).

Table 2. Summary of multivariate regressions for allometric variation of humeral shape based on Procrustes coordinates (*Pcoor*) on body mass (M_b) and centroid size (CS).

Linear Model	adj R^2	*p*-Value
CS	0.256	<0.001
M_b	0.121	<0.001

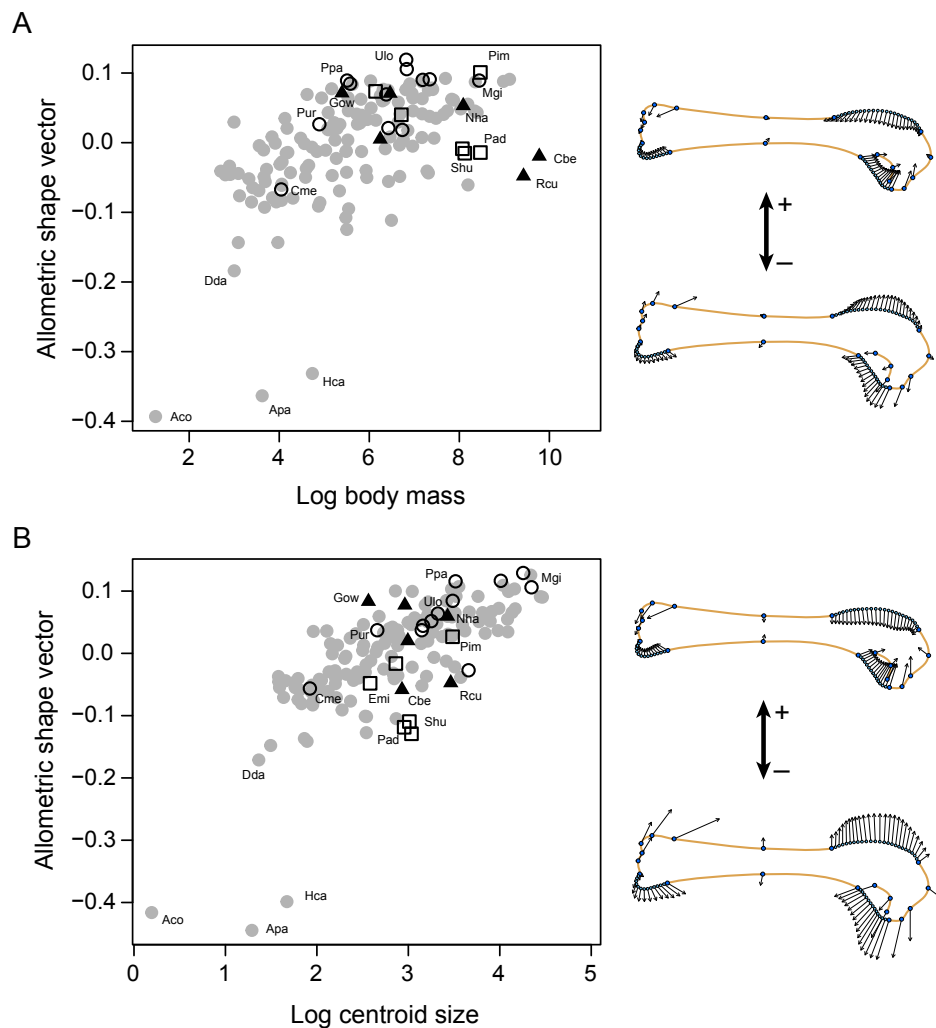| PGLS	adj R^2	*p*-Value
CS	0.058	<0.001
flighted-flightless	0.056	<0.001
CS: flighted-flightless	0.012	0.108
M_b	0.022	0.016
flighted-flightless	0.057	<0.001
M_b: flighted-flightless	0.014	0.074

Figure 5. Allometric scaling of the humeral shape (Procrustes coordinates) on both, body mass (**A**) and centroid size (**B**). Shape changes associated with each allometric vector are shown by vector graphs. Symbols' shape corresponds with the wing function provided in Figure 2. Abbreviations: Aco, *Archilochus colubris*; Apa, *Apus pacificus*; Cbe, *Casuarius bennetti*; Cme, *Cinclus mexicanus*; Dda, *Delichon dasypus*; Emi, *Eudyptula minor*; Gow, *Gallirallus owstoni*; Hca, *Hirundapus caudacutus*; Mgi, *Macronectes giganteus*; Nha, *Nannopterum harrisi*; Pad, *Pygoscelis adeliae*; Ppa, *Puffinus pacificus*; Pim, *Pinguinus impennis*; Pur, *Pelecanoides urinatrix*; Rcu, *Rapphus cucullatus*; Shu, *Spheniscus humboldti*; Ulo, *Uria lomvia*.

The two first principal components (PCs) capture 83.3% of the total morphological variation of the humerus in our sample. Mapping the phylogeny onto our PCA plot shows that Apodiformes (swifts and hummingbirds), Sphenisciformes (penguins) and some Alcidae (e.g., *Pinguinus*, *Mancalla*, *Uria*, and *Brachyramphus*) are very divergent in humeral shape from the rest of clades (Figure 6A). Shape change along PC1 (55.2% of the variance) depicts variations related with the general robustness of the bone associated with the expansion of both epiphyses and the shortening of the chord length of the diaphysis. Positive scores are associated with short and wide humeri (e.g., swifts and hummingbirds, penguins, swallows) while negative scores are associated with long and slender humeri (e.g., albatross and petrels, O. Procellariiformes). PC2 (28.1% of the variance) mainly describes differences in the proximodistal extension of the deltopectoral crest coupled with changes in the extension of the bicipital crest in the proximal epiphysis. Positive scores in PC2 are associated with distally expanded but dorsally shallow deltopectoral crests and a bicipital crest restricted to the proximal end of the humerus like in some penguins and some alcids, including the extinct flightless *P. impennis* and *M. milleri*, (Figure 6A). Negative scores along PC2 are associated with shorter and more dorsally projected deltopectoral crests,

and more ventrally expanded bicipital crests as shown by hummingbirds (Trochilidae) and, to a lesser degree, by swallows (Hirundinidae) and swifts (Apodidae).
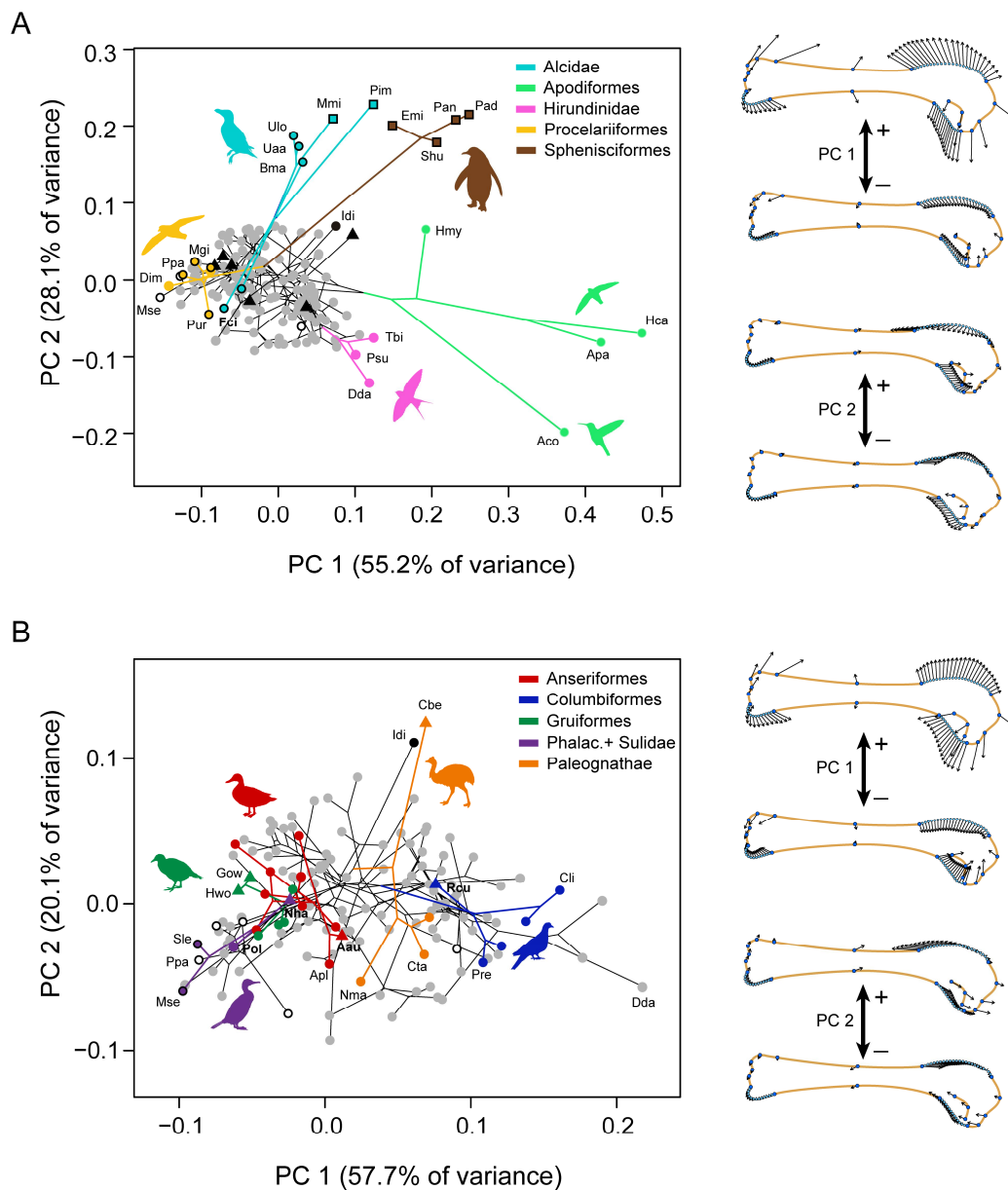

Figure 6. Allometric-free variation of humeral shape. (**A**) Phylomorphospace depicting the two first principal components of the PCA and vector graphs showing the shape changes associated with each of the axes. (**B**) Phylomorphospace depicted by the two first principal components of the PCA on the subsample excluding Apodiformes, Sphenisciformes and Alcidae, and vector graphs showing the shape changes. Symbols' shape corresponds with the function of wings given in Figure 2. Abbreviations: Aau, *Anas aucklandica*; Aco, *Archilochus colubris*; Apa, *Apus pacificus*; Apl, *Anas platyrhynchos*; Bma, *Brachyramphus marmoratus*; Cbe, *Casuarius bennetti*; Cli, *Columba livia*; Cta, *Crypturellus tataupa*; Dda, *Delichon dasypus*; Dim, *Diomedea inmutabilis*; Emi, *Eudyptula minor*; Fci, *Fratercula cirrhata*; Gow, *Gallirallus owstoni*; Hca, *Hirundapus caudacutus*; Hmy, *Hemiprocne mystacea*; Hwo, *Hypotaenidya woodfordi*; Idi, *Ichthyornis dispar*; Mmi, *Mancalla milleri*; Mgi, *Macronectes giganteus*; Mse, *Morus serrator*; Nha, *Nannopterum harrisi*; Nma, *Nothura maculosa*; Pad, *Pygoscelis adeliae*; Pan, *Pygoscelis antarctica*; Pim, *Pinguinus impennis*; Pol, *Phalacrocorax olivaceus*; Ppa, *Puffinus pacificus*; Pre, *Ptilinopus regina*; Psu, *Progne subis*; Pur, *Pelecanoides urinatrix*; Rcu, *Rapphus cucullatus*; Shu, *Spheniscus humboldti*; Sle, *Sula leucogaster*; Tbi, *Tachycineta bicolor*; Uaa, *Uria aalge*; Ulo, *Uria lomvia*.

Because the main axes of variation are created by shape differences among outlier taxa (i.e., Apodiformes, Sphenisciformes and Alcidae), we conducted a second PCA excluding these groups in order to observe the variation among the remaining species (Figure 6B). As in the first analysis, the shape captured by the new PC1 is associated with the robustness of the humerus related to the expansion of epiphyses and shortening of the diaphysis, while the new PC2 depicts differences in the length of the deltopectoral crest with respect to the proximal-distal position of the ventral region of the proximal epiphysis (including the bicipital crest). The non-neornithine *Ichthyornis dispar* scores in the extreme positive axis of the PC2 showing the ventral region located more proximally with respect a long deltopectoral crest (DPC) than the bulk of the other birds (Figure 6B). Compared to *Ichthyornis*, although there is some disparity between clades, most neornithines tend to increase the dorsoventral symmetry of the proximal epiphysis by restricting both deltopectoral crest and bicipital crest regions proximally. Abundant overlapping of branches within the central region of the morphospace (Figure 6A,B) seems to indicate that these morphologies have been explored several times during neornithine evolution. This is confirmed by a significant value of $K_{mult} = 1.48$, indicating overall higher similarity among related taxa than expected ($p < 0.001$). However, when the most divergent lineages are not considered, a value close to expectations of Brownian motion is recovered ($K_{mult} = 1.04$; $p = 0.02$).

Within Paleognathae, the humerus of the flightless cassowary (*Casuarius bennetti*) shows a morphological trend close to *Ichthyornis*, while flying tinamous show morphologies much more similar to other neornithines. Within Neognathae, flightless taxa (i.e., *Anas aucklandica*, *Rapphus cucullatus*, *Gallirallus owstoni*, *Hypotaenidya woodfordi*, and *Nannopterum harrisi*) do not seem to follow a common morphological trend though (Figure 6B). Flightless rails (*G. owstoni*, *H. woodfordi*) and the Dodo (*R. cucullatus*) have humeri lesser robust than their flying counterparts from Gruiformes and Columbiformes, respectively. In contrast, the flightless cormorant (*N. harrisi*) increases the humeral robustness, distally lengthens the DPC and locates the ventral epiphysis more proximal with respect to its closest relatives. The Auckland Teal (*A. aucklandica*) shows a similar morphology than the flying mallard (*Anas platyrhynchos*).

4. Discussion

In agreement with previous studies [27,29,30] linear size metrics of the humerus (i.e., humeral length, *HL* and humeral width, *HW*) scale with body mass (M_b) according with allometric factors of 0.42 and 0.36, respectively. Meanwhile when only the flying subsample is accounted for, the scaling factors increase slightly (i.e., 0.48 and 0.38), remaining above the expected slope of isometry (i.e., 0.33), that is, humerus dimensions increase faster than body mass and length of the humerus increases faster with body mass than the width of the humeral diaphysis (Table 1, Figure 4) [30]. This entails that as body mass increases the humerus of flying birds tend to be longer and thinner. In flightless birds, however, the slopes for both variables are lower than expected for isometry (*HL* slope = 0.14; *HW* slope = 0.29) meaning that body mass increases faster than humeral dimensions and the humerus of flightless birds tends to be shorter and thicker in heavier birds. We also found that centroid size (*CS*; i.e., the our humeral size proxy) is closely associated with *HL*, but not with *HW*, suggesting the *CS* calculation for birds' humerus is much more influenced by length than by width, and revealing once again the skewness *CS* can produce towards certain variations in geometry (e.g., [18,54]).

In agreement with our results on linear allometry, shape allometric variation related with both size proxies, *CS* and M_b, mainly reflects variations in the robustness of the humerus (i.e., larger humeri or heavier birds are associated with less robust humeri; Figure 5). This is also consistent with previous studies suggesting bone length increases faster than shaft diameter in large birds [27,30,55]. We found that this allometric variation is not a dominant factor of the morphological variability in the humerus of birds as a single group (i.e., 2–6% of bone shape variance), but most of this allometric variation is due to differences in size and shape (e.g., clades with large and slender humeri vs. clades with small and robust humeri) as revealed by the shape variance explained by size variations using non-phylogenetic

models (i.e., 25–29%; Table 2). Surprisingly, allometric trends of flightless and flighted birds with *CS* and M_b were not statistically different (Table 1), although this signification should be taken cautiously, especially in the case of M_b ($p = 0.074$), as the non-parametric Procrustes ANOVAs might increase the likelihood of a type II error in samples with heterogeneity of within-group variance [51] as ours. In addition, flightless birds seem to follow an opposite tendency in which their humeri become more robust as M_b increases (Figure 5A), which is also consistent with the scaling of *HL* and *HW* reported above (Figure 4, Table 1). These results reveal the primal influence of flight adaptation in humeral allometry in modern birds.

However, the link between morphological variations of the humerus and its more specific locomotory functions in birds is intricate. More than 80% of the allometric-free variation reflects changes in the bone robustness associated with the expansion of the epiphyses and shortening of the diaphysis (i.e., PC1), as well as in the relative development of the dorsal and ventral crests in the proximal epiphysis (i.e., PC2). These morphological variations are highly related to the capacity of the bone to bear stresses [8,10] and wing's mechanics [56–58]. The humeral morphology displayed here by the Upper Cretaceous ornithurine *Ichthyornis dispar* (Figure 6) can be seen in other non-neornithine ornithuromorphs (e.g., [25]). Comparisons of morphological disparity of the humerus in the crown group of birds (i.e., Neornithes) with such pre-neornithine condition illustrate that the humerus of the majority of living bird lineages tended towards a configuration with proximally restricted deltopectoral crests (DPC), that is, closer to the glenoid joint, while more distally located bicipital crests (BC), that is further from the glenoid (Figure 6). Such a configuration implies, on the one hand, a DPC that enhances faster movements of the wing and less contraction length of the pectoralis fibers, and on the other, a biceps closer to elbow and, then with shorter fibers that can exert more force (see [56,59,60]). As a result, we suggest that this morphological transformation of the humerus involved an improvement to flap efficiently in neornithines and likely represents a functional optimum that constrains the evolution of humeral morphology in most neornithines lineages. In addition, developmental constraints could have also played a role in restricting shape variation of the humerus in many neornithine lineages. Quantitative measures of similarity indicate that this constrained pattern is true when all neornithines are considered ($K_{mult} = 1.48$), and we found evidence for two functional regimes which deviate from this general morphological trend, which are both the result of a secondary specialization to a highly stressful wing-propelled locomotion in a handful of lineages: intense aerial flapping and underwater wing propulsion. However, when lineages of these two outlier cases are excluded, quantitative measures suggest that within the rest of neornithines, there is significant variation in shape that adjust well to Brownian Motion model of evolution within an specific region of the shape space ($K_{mult} = 1.04$).

Apodiformes stand among the lineages which developed an intense aerial flapping activity, as swifts are hyperaerials (i.e., they spend almost their entire life airborne, roosting, mating and foraging) and hummingbirds are the only birds capable of prolonged hovering (i.e., a flight style that requires a very high frequency of flapping because the lift generation comes entirely from the flapping wings) [61–63]. These birds display extremely robust humeri (Figure 6A) that allow to deal with the high stresses generated on their wings—that have proportionality very long handwings [62]—from either, hyperariality or prolonged hovering. Their humeri also differ from the remaining of birds in the shape of the proximal epiphysis—DPC is very short and dorsally projected, and the BC lengthens distally—, what is especially conspicuous in hummingbirds (Figure 6A). The shortening of the DPC increases the mechanical advantage of the pectoral and deltoids muscles to achieve faster wing strokes (see [58,60]), while the lengthening of the BC is consistent with a well-developed biceps and the fact of hummingbirds keep the elbow flexed during the full wing cycle [62]. The humeral morphology of hirundinid passerines (i.e., martins and swallows) displays an incipient pattern of homoplasy in the humeral shape with Apodiformes (Figure 6A), which is consistent with other similarities regarding wing shape, wing loading, and hyperaerial habits [64–66].

On the other hand, underwater wing propulsion is highly stressful for the wings as the fluid forces (i.e., lift and drag) in the water are four times those undergone in the air at the same Reynolds number [67]. Wing-propelled diving has evolved at least five times within neornithines: in penguins (Sphenisciformes), auks (Alcidae), petrels and shearwaters (Procellariidae), diving-petrels (Pelecanoididae), dippers (Cinclidae), and extinct plotopterids (Plotopteridae). Among them, penguins and plotopterids, which might be closely related [68], are the only clades that lost the flight capacity and fully adapted to underwater foraging [6,43,69]. Compared to close flighted relatives and the bulk of modern birds, penguins have humeri with very long DPCs and reduced BCs (Figure 6A). As pectoralis, supracoracoideus and deltoids muscles are inserted only on the most proximal region of the DPC [70], the length of this crest would not reflect the mechanical advantage of flapping as we have previously described. Meanwhile, the reduced BC reflects the loss of the biceps and the minimal elbow mobility in penguins [69]. The stiffening of the wing of penguins to serve as a flipper have involved the further loss or reduction of forelimb muscles and the movement restriction of the rest of joints [69,70]. Our results support that these modifications to make the wing stiffer are linked to a high robustness of the humerus in the craniocaudal axis (Figure 6A). We therefore suggest that this robust humerus is well-suited to resist the high stresses supported by the wing as a consequence of the high loadings imposed by the fluid forces of water [71]. The extinct species of Alcidae, *P. impennis* and *M. milleri*, show seemingly convergent humeral morphologies with penguins (Figure 6A), which is in agreement with another anatomical features indicating they were flightless wing-propelled divers (e.g., [7,43,72,73]). Extant alcids are capable of both wing-propelled flying and diving. Surprisingly, we have identified humeral shape disparity among them, which as far as we know has been previously overlooked. The morphology of genera *Uria* and *Brachyramphus* closely approach that of extinct flightless *Pinguinnus* and *Mancalla*, showing higher robustness and much longer DPC than genera *Fratercula* and *Cepphus* (Figure 1F–G, Figure 6A). Such a divergent pattern within Alcidae could indicate that some species improve flapping capacity in air, while others improve it in the water; although this issue needs to be farther explored on a study focused on alcids. Similarly to *Fratercula* and *Cepphus*, the other modern taxa that evolved underwater wing propulsion together with flying capacity (i.e., Procellariidae, Pelecanoididae and Cinclidae) have a humeral morphology that does not differ significantly from the bulk of Neornithes (Figure 6A). Consistently with [6], this result indicate that the aquatic medium imposes extreme selective pressures on the morphology. Hence, the idea that the lineages of alcids and penguins exhibit an aerial-diving functional trade-off of the wing [74] would imply that the transition to a more frequent aquatic wing propelled locomotion would involve greater morphological changes than the transition to a more frequent use of aerial locomotion. However, the flighted species of these lineages should not be viewed as steps of an evolutionary trajectory towards the loss of flight [43].

Our results also show that the loss of wing function in different lineages of neornithines involved divergences in humeral shape from their flying closest relatives (Figure 6B). However, a morphological trend common to all these flightless lineages was not found. The morphological pattern observed in birds that completely loss the wing function responds to three different scenarios: (1) Long-time flightless lineages as the cassowary that show a clear regression to the plesiomorphic morphology with regards to flying relatives. To extend this result to other flightless paleognaths as ostriches and rheas further analysis is necessary, as their humeri are very different from that of the cassowary and could not be analyzed (see material and methods); (2) Terrestrial flightless birds inhabiting small islands without predators, as the extinct dodo (*R. cucullatus*) and the rails from Pacific Islands (e.g., *H. woodfordi*, *G. owstoni*), which tend to decrease the humeral robustness with respect to their relatives; (3) a combination of island isolation and foot-propelling aquatic locomotion, such are cases of the Auckland teal (*A. aucklandica*) and the flightless cormorant (*N. harrisi*). The humerus of the former did not greatly diverge from *A. platyrrhynchos*, its closest relative analyzed, while the humerus of the latter increased its robustness and acquired a more plesiomorphic condition for the proximal epiphysis, with respect to flying cormorants and other close relatives. This might be related with a more recent

divergence of the Auckland teal from its flighted counterparts than the flightless cormorant [75,76] although this has not been tested in detail yet.

The absence of a common morphological pattern in birds without locomotory wing function may reflect that the relaxation of functional flight constraints could entail unpredictable morphological variations of the humerus that can lead to different trends including an apparent reversal towards the plesiomorphic condition (as observed for the cassowary, dodo, and flightless cormorant, but not for rails). The release of these functional constraints do not necessarily imply that functional pressures do not affect the morphology of the humerus in these taxa. For instance, while the wing of flightless cormorant is reduced with respect to its flying relatives [77], the humerus increases in robustness (Figure 6B). This change could reflect a skeletal modification to make the bone denser, which would be consistent with the increase of body mass and other anatomical modifications that reduce the buoyancy enhancing its subaquatic performance [77–80].

5. Conclusions

Our results support that: (1) locomotory adaptation is an important factor shaping the evolution of the morphological disparity of the humerus in Neornithes; (2) allometric variation is unexpectedly low and shows an opposite pattern in flighted birds to that of flightless birds, particularly in relation with the robustness of this bone; (3) considering the humeral morphology of *Ichthyornis* and other non-neornithine ornithuromorphs [25] as plesiomorphic, we suggest that the transformations in the proximal epiphysis in neornithines would have entailed an improvement in the flapping efficiency in the clade; (4) extreme adaptation to highly stressful wing-propelled locomotion in air (swifts and hummingbirds) and water (penguins and some auks) results in the main morphological divergences observed among neornithines, and in both cases, involves a very robust humeral morphology; (5) the disparity between flighted and flightless wing-propelled divers supports previous hypotheses [6] suggesting that the transition from a "double" wing use (both flying and diving) condition to a fully aquatic use condition involves greater changes than the transition from a purely aerial locomotory condition to a "double" wing use condition; and (6) a common morphological pattern associated with the loss of locomotory function of the wing was not found, what implies the relaxation of the constraints imposed by flapping in fluids on the humerus do not have a predictive effect in the evolution of the architecture of this bone.

Although focused on the two-dimensional shape of the bone and other attributes of morphological variation in the humerus, our study represents one of the first steps towards the understanding of the evolution of postcranial anatomy among the whole extant radiation of birds. In addition, we raise several issues regarding the disparity of the avian humerus and provides a framewrok for future analyses at a broad scale and focuses in clade specific trends which deserve further study (e.g., alcids, paleognaths, and cormorants).

Author Contributions: Conceptualization, F.J.S. and M.C.-P.; Methodology, F.J.S. and A.M.-S.; Formal Analysis, F.J.S., M.C.-P. and A.M.-S.; Investigation, F.J.S., M.C.-P. and G.N.; Data Curation, F.J.S., and A.M.-S.; Writing—Original Draft Preparation, F.J.S. and M.C.-P.; Writing—Review & Editing, F.J.S., A.M.-S. and G.N.; Visualization, F.J.S., A.M.-S. and G.N. All authors have read and agreed to the published version of the manuscript.

Conflicts of Interest: The authors declare no conflict of interest.

References

1. Barrowclough, G.F.; Cracraft, J.; Klicka, J.; Zink, R.M. How many kinds of birds are there and why does it matter? *PLoS ONE* **2016**, *11*, e0166307. [CrossRef] [PubMed]

2. Norberg, U.L. Flight and scaling of flyers in nature. *Flow Phenom. Nat.* **2007**, *1*, 120–154.

3. Butler, P.J. The physiological basis of bird flight. *Philos. Trans. R. Soc. B Biol. Sci.* **2016**, *371*, 20150384. [CrossRef] [PubMed]

4. Tobalske, B.W. Avian Flight. In *Handbook of Bird Biology*, 3rd ed.; Lovette, I.J., Fitzpatrick, J.W., Eds.; Wiley-Blackwell: The Cornell Lab of Ornithology: Ithaca, NY, USA, 2016; pp. 149–169.

5. Pennycuick, C.J. *Modelling the Flying Bird*, 1st ed.; AP Theoretical Ecology Series; Academic Press: Oxford, UK, 2008; Volume 5, p. 496.

6. Habib, M. The structural mechanics and evolution of aquaflying birds. *Biol. J. Linn. Soc.* **2010**, *99*, 687–698. [CrossRef]

7. Smith, N.A.; Clarke, J.A. Osteological histology of the Pan-Alcidae (Aves, Charadriiformes): Correlates of wing-propelled diving and flightlessness. *Anat. Rec.* **2014**, *297*, 188–199. [CrossRef]

8. De Margerie, E.; Sanchez, S.; Cubo, J.; Castanet, J. Torsional resistance as a principal component of the structural design of long bones: Comparative multivariate evidence in birds. *Anat. Record Part A* **2005**, *282*, 49–66.

9. Nudds, R.L.; Dyke, G.J.; Rayner, J.M.V. Avian brachial index and wing kinematics: Putting movement back into bones. *J. Zool.* **2007**, *272*, 218–226. [CrossRef]

10. Habib, M.B.; Ruff, C. The effects of locomotion on the structural characteristics of avian limb bones. *Zool. J. Linn. Soc.* **2008**, *153*, 601–624. [CrossRef]

11. Simons, E.L.; Hieronymus, T.L.; O'Connor, P.M. Cross sectional geometry of the forelimb skeleton and flight mode in pelecaniform birds. *J. Morphol.* **2011**, *272*, 958–971. [CrossRef]

12. Raikow, R.J. Locomotor system. In *Form and Function in Birds*; King, A.S., McLellan, J., Eds.; Academic Press: Cambridge, MA, USA, 1985; Volume 3, pp. 57–147.

13. Baumel, J.J.; King, A.S.; Breazile, J.; Evans, H.; Vanden Berge, J.C. *Handbook of Avian Anatomy: Nomina Anatomica Avium*, 2nd ed.; Harvard Univ Nuttall Ornithological Club: Cambridge, MA, USA, 1993; p. 779.

14. Bright, J.A.; Marugán-Lobón, J.; Cobb, S.N.; Rayfield, E.J. The shapes of bird beaks are highly controlled by nondietary factors. *Proc. Natl. Acad. Sci. USA* **2016**, *113*, 5352–5357. [CrossRef]

15. Marugán-Lobón, J.; Watanabe, A.; Kawabe, S. Studying avian encephalization with geometric morphometrics. *J. Anat.* **2016**, *229*, 191–203. [CrossRef] [PubMed]

16. Cooney, C.R.; Bright, J.A.; Capp, E.J.; Chira, A.M.; Hughes, E.C.; Moody, C.J.; Nouri, L.O.; Varley, Z.K.; Thomas, G.H. Mega-evolutionary dynamics of the adaptive radiation of birds. *Nature* **2017**, *542*, 344–347. [CrossRef] [PubMed]

17. Felice, R.N.; Goswami, A. Developmental origins of mosaic evolution in the avian cranium. *Proc. Natl. Acad. Sci. USA* **2018**, *115*, 555–560. [CrossRef] [PubMed]

18. Navalón, G.; Bright, J.A.; Marugán-Lobón, J.; Rayfield, E.J. The evolutionary relationship among beak shape, mechanical advantage, and feeding ecology in modern birds. *Evolution* **2019**, *73*, 422–435. [CrossRef] [PubMed]

19. Navalón, G.; Marugán-Lobón, J.; Bright, J.A.; Cooney, C.R.; Rayfield, E.J. The consequences of craniofacial integration for the adaptive radiations of Darwin's finches and Hawaiian honeycreepers. *Nat. Ecol. Evol.* **2020**, *4*, 270–278. [CrossRef] [PubMed]

20. Shatkovska, O.V.; Ghazali, M. Integration of skeletal traits in some passerines: Impact (or the lack thereof) of body mass, phylogeny, diet and habitat. *J. Anat.* **2020**, *236*, 274–287. [CrossRef]

21. Close, R.A.; Rayfield, E.J. Functional morphometric analysis of the furcula in Mesozoic birds. *PLoS ONE* **2012**, *7*, e36664. [CrossRef]

22. Wang, X.; Clarke, J.A. The evolution of avian wing shape and previously unrecognized trends in covert feathering. *Proc. R. Soc. B Biol. Sci.* **2015**, *282*, 20151935. [CrossRef]

23. Watanabe, J. Clade-specific evolutionary diversification along ontogenetic major axes in avian limb skeleton. *Evolution* **2018**, *72*, 2632–2652. [CrossRef]

24. Nebreda, S.M.; Navalón, G.; Menéndez, I.; Sigurdsen, T.; Chiappe, L.M.; Marugán-Lobón, J. Disparity and macroevolutionary transformation of the maniraptoran manus. *Bull. Am. Mus. Nat. Hist.* in press.

25. Navalón, G.; Meng, Q.; Marugán-Lobón, J.; Zhang, Y.; Wang, B.; Xing, H.; Liu, D.; Chiappe, L. Diversity and evolution of the Confuciusornithidae: Evidence from a new 131-million-year-old specimen from the Huajiying Formation in NE China. *J. Asian Earth Sci.* **2018**, *152*, 12–22. [CrossRef]

26. Mayr, G. *Avian Evolution: The Fossil Record of Birds and its Paleobiological Significance*; John Wiley and Sons: Chichester, UK, 2017; p. 306.

27. Olmos, M.; Casinos, A.; Cubo, J. Limb allometry in birds. *Annales des Sciences Naturelles-Zoologie et Biologie Animale* **1996**, *17*, 39–49.

28. Cubo, J.; Casinos, A. Biomechanical significance of cross-sectional geometry of avian long bones. *Eur. J. Morphol.* **1998**, *36*, 19–28. [CrossRef] [PubMed]

29. Nudds, R.L. Wing-bone length allometry in birds. *J. Avian Biol.* **2007**, *38*, 515–519. [CrossRef]

30. Sullivan, T.N.; Meyers, M.A.; Arzt, E. Scaling of bird wings and feathers for efficient flight. *Sci. Adv.* **2019**, *5*, eaat4269. [CrossRef]

31. Sievwright, H.; Macleod, N. Eigensurface analysis, ecology, and modelling of morphological adaptation in the falconiform humerus (Falconiformes: Aves). *Zool. J. Linn. Soc.* **2012**, *165*, 390–419. [CrossRef]

32. Adams, D.C.; Rohlf, F.J.; Slice, D.E. A field comes of age: Geometric morphometrics in the 21st century. *Hystrix* **2013**, *24*, 7.

33. Prum, R.O.; Berv, J.S.; Dornburg, A.; Field, D.J.; Townsend, J.P.; Lemmon, E.M.; Lemmon, A.R. A comprehensive phylogeny of birds (Aves) using targeted next-generation DNA sequencing. *Nature* **2015**, *526*, 569–573. [CrossRef]

34. Marugán-Lobón, J.; Buscalioni, A.D. Geometric morphometrics in macroevolution: Morphological diversity of the skull in modern avian form in contrast to some theropods dinosaurs. In *Morphometrics: Applications in Biology and Paleontology*; Elewa, A., Ed.; Springer: New York, NY, USA, 2004; pp. 157–171.

35. Hume, J.P.; Steel, L. Fight club: A unique weapon in the wing of the solitaire, *Pezophaps solitaria* (Aves: Columbidae), an extinct flightless bird from Rodrigues, Mascarene Islands. *Biol. J. Linn. Soc.* **2013**, *110*, 32–44. [CrossRef]

36. Clarke, J.A. Morphology, phylogenetic taxonomy, and systematics of *Ichthyornis* and *Apatornis* (Avialae: Ornithurae). *Bull. Am. Mus. Nat. Hist.* **2004**, *286*, 1–179. [CrossRef]

37. Porras-Múzquiz, H.G.; Chatterjee, S.; Lehman, T.M. The carinate bird *Ichthyornis* from the Upper Cretaceous of Mexico. *Cretac. Res.* **2014**, *51*, 148–152. [CrossRef]

38. Maddison, W.P.; Maddison, D.R. Mesquite: A Modular System for Evolutionary Analysis. Version 3.5. 2011. Available online: http://mesquiteproject.org (accessed on 1 April 2020).

39. Kumar, S.; Stecher, G.; Suleski, M.; Hedges, S.B. TimeTree: A resource for timelines, timetrees, and divergence times. *Mol. Biol. Evol.* **2017**, *34*, 1812–1819. [CrossRef] [PubMed]

40. Del Hoyo, J.; Elliott, A.; Sargatal, J.; Christie, D.A.; Kirwan, G. (Eds.) *Handbook of the Birds of the World Alive*; Lynx Edicions: Barcelona, Spain, 2020. Available online: http://www.hbw.com/ (accessed on 1 April 2020).

41. Myers, P.; Espinosa, R.; Parr, C.S.; Jones, T.; Hammond, G.S.; Dewey, T.A. The Animal Diversity Web (online). 2020. Available online: https://animaldiversity.org (accessed on 1 April 2020).

42. Serrano, F.J.; Palmqvist, P.; Sanz, J.L. Multivariate analysis of neognath skeletal measurements: Implications for body mass estimation in Mesozoic birds. *Zool. J. Linn. Soc.* **2015**, *173*, 929–955. [CrossRef]

43. Smith, N.A. Evolution of body mass in the Pan-Alcidae (Aves, Charadriiformes): The effects of combining neontological and paleontological data. *Paleobiology* **2016**, *42*, 8–26. [CrossRef]

44. Howard, H. A review of the extinct avian genus, *Mancalla*. *Los Angel. Cty. Mus. Contrib. Sci.* **1970**, *203*, 1–12.

45. van Heteren, A.H.; van Dierendonck, R.C.; van Egmond, M.A.; Sjang, L.; Kreuning, J. Neither slim nor fat: Estimating the mass of the dodo (*Raphus cucullatus*, Aves, Columbiformes) based on the largest sample of dodo bones to date. *PeerJ* **2017**, *5*, e4110. [CrossRef]

46. Rohlf, F.J. *TPS Dig v.2.25*; Department of Ecology and Evolution, State University of New York: Stony Brook, NY, USA, 2016. Available online: http://life.bio.sunysb.edu/morph/ (accessed on 1 April 2020).

47. R Core Team. *R: A Language and Environment for Statistical Computing*; Version 3.4.1; R Foundation for Statistical Computing: Vienna, Austria, 2017. Available online: http://cran.R-project.org (accessed on 1 April 2020).

48. Adams, D.C.; Collyer, M.; Kaliontzopoulou, A.; Sherratt, E. Geomorph: Software for Geometric Morphometric Analyses. 2016. Available online: https://cran.r-project.org/web/packages/geomorph/index.html (accessed on 1 April 2020).

49. Dryden, I.L.; Mardia, K. *Statistical Analysis of Shape*; Wiley: Chichester, UK, 1998; p. 347.

50. Gunz, P.; Mitteroecker, P. Semilandmarks: A method for quantifying curves and surfaces. *Hystrix* **2013**, *24*, 103–109.

51. Collyer, M.L.; Sekora, D.J.; Adams, D.C. A method for analysis of phenotypic change for phenotypes described by high-dimensional data. *Heredity* **2015**, *115*, 357–365. [CrossRef]

52. Revell, L.J. Phytools: An R package for phylogenetic comparative biology (and other things). *Methods Ecol. Evol.* **2012**, *3*, 217–223. [CrossRef]

53. Maddison, W.P. Squared-change parsimony reconstructions of ancestral states for continuous-valued characters on a phylogenetic tree. *Syst. Biol.* **1991**, *40*, 304–314. [CrossRef]

54. Kulemeyer, C.; Asbahr, K.; Gunz, P.; Frahnert, S.; Bairlein, F. Functional morphology and integration of corvid skulls–a 3D geometric morphometric approach. *Front. Zool.* **2009**, *6*, 2. [CrossRef] [PubMed]

55. Cubo, J.; Casinos, A. Scaling of skeletal element mass in birds. *Belg. J. Zool.* **1994**, *124*, 127–137.

56. Baier, D.B.; Gatesy, S.M.; Jenkins, F.A. A critical ligamentous mechanism in the evolution of avian flight. *Nature* **2007**, *445*, 307–310. [CrossRef]

57. Tobalske, B.W.; Warrick, D.R.; Jackson, B.E.; Dial, K.P. Morphological and Behavioral Correlates of Flapping Flight. In *Living Dinosaurs: The Evolutionary History of Modern Birds*; Dyke, G., Kaiser, G., Eds.; Wiley-Blackwell: Hoboken, NJ, USA, 2011; pp. 257–281.

58. Serrano, F.J.; Chiappe, L.M. Aerodynamic modelling of a Cretaceous bird reveals thermal soaring capabilities during early avian evolution. *J. R. Soc. Interface* **2017**, *14*, 20170182. [CrossRef] [PubMed]

59. Hildebrand, M.; Goslow, G.E. *Analysis of vertebrate structure*, 5th ed.; John Wiley & Sons: New York, NY, USA, 2001; p. 656.

60. Alexander, R.M. *Principles of Animal Locomotion*; Princeton University Press: Princeton, NJ, USA, 2003; p. 384.

61. Chai, P.; Millard, D. Flight and size constraints: Hovering performance of large hummingbirds under maximal loading. *J. Exp. Biol.* **1997**, *200*, 2757–2763.

62. Videler, J.J. Avian Flight. In *Oxford Ornithology Series*; Birkhead, T.R., Ed.; Oxford University Press: Oxford, UK, 2006; p. 288.

63. Karkhu, A.A. Morphological divergence within the order Apodiformes as revealed by the structure of the humerus. *Natur. Hist. Mus. Los Angel. Co. Sci. Ser.* **1992**, *36*, 379–384.

64. Savile, D.B.O. Adaptive evolution in the avian wing. *Evolution* **1957**, *11*, 212–224. [CrossRef]

65. Rayner, J.M. Form and function in avian flight. In *Current Ornithology*; Springer: Berlin/Heidelberg, Germany, 1988; pp. 1–66.

66. Turner, A. Swallows and Martins (Hirundinidae). In *Handbook of the Birds of the World Alive*; del Hoyo, J., Elliott, A., Sargatal, J., Christie, D.A., de Juana, E., Eds.; Lynx Edicions: Barcelona, Spain, 2020; Available online: https://www.hbw.com/node/52303 (accessed on 28 February 2020).

67. Johansson, L.C.; Aldrin, B.S.W. Kinematics of diving Atlantic puffins (*Fratercula arctica* L.): Evidence for an active upstroke. *J. Exp. Biol.* **2002**, *205*, 371–378.

68. Mayr, G. Tertiary plotopterids (Aves, Plotopteridae) and a novel hypothesis on the phylogenetic relationships of penguins (Spheniscidae). *J. Zool. Syst.* **2005**, *43*, 67–71. [CrossRef]

69. Raikow, R.J.; Bicanovsky, L.; Bledsoe, A.H. Forelimb joint mobility and the evolution of wing-propelled diving in birds. *Auk* **1988**, *105*, 446–451. [CrossRef]

70. Louw, G.J. Functional anatomy of the penguin flipper. *J. S. Afr. Vet. Assoc.* **1992**, *63*, 113–120.

71. Lovvorn, J.R.; Liggins, G.A. Interactions of body shape, body size and stroke-acceleration patterns in costs of underwater swimming by birds. *Funct. Ecol.* **2002**, *16*, 106–112. [CrossRef]

72. Livezey, B.C. Morphometrics of flightlessness in the Alcidae. *Auk* **1988**, *105*, 681–698. [CrossRef]

73. Smith, N.A. Taxonomic revision and phylogenetic analysis of the flightless Mancallinae (Aves, Pan-Alcidae). *ZooKeys* **2011**, *91*, 1–116. [CrossRef] [PubMed]

74. Elliott, K.H.; Ricklefs, R.E.; Gaston, A.J.; Hatch, S.A.; Speakman, J.R.; Davoren, G.K. High flight costs, but low dive costs, in auks support the biomechanical hypothesis for flightlessness in penguins. *Proc. Natl. Acad. Sci. USA* **2013**, *110*, 9380–9384. [CrossRef] [PubMed]

75. Jetz, W.; Thomas, G.H.; Joy, J.B.; Hartmann, K.; Mooers, A.O. The global diversity of birds in space and time. *Nature* **2012**, *491*, 444–448. [CrossRef] [PubMed]

76. Mitchell, K.J.; Wood, J.R.; Scofield, R.P.; Llamas, B.; Cooper, A. Ancient mitochondrial genome reveals unsuspected taxonomic affinity of the extinct Chatham duck (*Pachyanas chathamica*) and resolves divergence times for New Zealand and sub-Antarctic brown teals. *Mol. Phylogenet. Evol.* **2014**, *70*, 420–428. [CrossRef]

77. Livezey, B.C. Flightlessness in the Galápagos cormorant (*Compsohalieus* [*Nannopterum*] *harrisi*): Heterochrony, giantism and specialization. *Zool. J. Linn. Soc.* **1992**, *105*, 155–224. [CrossRef]

78. Wilson, R.P.; Hustler, K.; Ryan, P.G.; Burger, A.E.; Noldeke, E.C. Diving birds in cold water: Do Archimedes and Boyle determine energetic costs? *Am. Nat.* **1992**, *140*, 179–200. [CrossRef]

79. Halsey, L.G.; Blackburn, T.M.; Butler, P.J. A comparative analysis of the diving behaviour of birds and mammals. *Funct. Ecol.* **2006**, *20*, 889–899. [CrossRef]

80. Wilson, R.P.; Vargas, F.H.; Steinfurth, A.; Riordan, P.; Ropert-Coudert, Y.; Macdonald, D.W. What grounds some birds for life? Movement and diving in the sexually dimorphic Galapagos cormorant. *Ecol. Monogr.* **2008**, *78*, 633–652. [CrossRef]